

Polar landmark protein HubP recruits flagella assembly protein FapA under glucose limitation in *Vibrio vulnificus*

Soyoung Park,^{1,†‡} Jihee Yoon,^{2‡} Chang-Ro Lee,³
Ju Yeon Lee,⁴ Yeon-Ran Kim,¹ Kyoung-Soon Jang,⁴
Kyu-Ho Lee⁵ and Yeong-Jae Seok ^{1,2*}

¹School of Biological Sciences and Institute of Microbiology, Seoul National University, Seoul 08826, Republic of Korea.

²Department of Biophysics and Chemical Biology, Seoul National University, Seoul 08826, Republic of Korea.

³Department of Biological Sciences, Myongji University, Yongin 17058, Republic of Korea.

⁴Biomedical Omics Group, Korea Basic Science Institute, Cheongju 28119, Republic of Korea.

⁵Department of Biological Sciences, Sogang University, Seoul 04107, Republic of Korea.

Summary

How motile bacteria recognize their environment and decide whether to stay or navigate toward more favorable location is a fundamental issue in survival. The flagellum is an elaborate molecular device responsible for bacterial locomotion, and the flagellum-driven motility allows bacteria to move themselves to the appropriate location at the right time. Here, we identify the polar landmark protein HubP as a modulator of polar flagellation that recruits the flagellar assembly protein FapA to the old cell pole, thereby controlling its activity for the early events of flagellar assembly in *Vibrio vulnificus*. We show that dephosphorylated EIIA^{Glc} of the PEP-dependent sugar transporting phosphotransferase system sequesters FapA from HubP in response to glucose and hence inhibits FapA-mediated flagellation. Thus, flagellar assembly and motility is governed by spatiotemporal control of FapA, which is orchestrated by the competition between dephosphorylated EIIA^{Glc} and HubP, in the human pathogen *V. vulnificus*.

Accepted 30 April, 2019. *For correspondence. E-mail: yjseok@snu.ac.kr; Tel.: (+82) 2 880 4414; Fax: (+82) 2 888 4911 Present address: [†]Department of Biological Science, Binghamton Biofilm Research Center, Binghamton University, Binghamton, New York USA. [‡]These authors equally contributed to this work.

Introduction

Despite their structural simplicity, the bacterial cytoplasm is highly organized. Within the cytoplasm, cellular components can display distinct patterns of subcellular arrangements which are critical for various aspects of bacterial physiology and response to external environments (Laloux and Jacobs-Wagner, 2014; Treuner-Lange and Søgaard-Andersen, 2014). The rounded ends of rod-shaped bacteria, cell poles, constitute one of the fundamental subcellular domains for cellular processes such as cell cycle regulation, chemotaxis and flagellar motility.

To adapt and survive in changing environments, bacteria have to make the right decision to stay or move. Bacterial motility allows them to move toward favorable or away from unfavorable environments. The bacterial flagellum is a filamentous organelle which acts as a helical propeller and facilitates efficient locomotion (Chevance and Hughes, 2008). The complete flagellar machinery is composed of three major parts: the basal body (the engine and the export apparatus) and the hook and filament structures extending toward the extracellular space. From an architectural perspective, various proteins need to come together in a highly ordered flagellar assembly process which starts at the inner structure of the basal body then proceeds to the outer ones, and sophisticated transcriptional regulation mechanisms have been evolved to ensure the timely expression of subsets of flagellar genes. Although the flagellar structure, function of the flagellar genes and proteins, and their regulatory mechanisms are fairly conserved and well characterized in several motile bacteria (Francis *et al.*, 1994; McCarter, 2001; Terashima *et al.*, 2013; Minamino and Imada, 2015), the flagellation patterns such as the location and the number are diverse among bacterial species. Well-characterized examples of the flagellation patterns are peritrichous (many flagella along the lateral side, e.g., *Bacillus subtilis*, *Escherichia coli*), monotrichous (a single flagellum at one pole, e.g., *Caulobacter*, *Pseudomonas*, *Shewanella*, *Vibrio*), amphitrichous (bipolar flagella, e.g., *Campylobacter*) and lophotrichous (some flagella at one pole, e.g., *Helicobacter*) (Schuhmacher *et al.*, 2015).

Vibrio vulnificus, a rod-shaped Gram-negative bacterium, is an opportunistic human pathogen that possesses

a single polar flagellum. FapA (flagellar assembly protein A) has been identified as a glucose-responsive determinant of the polar localization and assembly of the single flagellum in *V. vulnificus* (Park *et al.*, 2016). In the presence of glucose, FapA interacts directly with dephosphorylated glucose-specific enzyme IIA (EIIA^{Glc}) of the phosphoenolpyruvate (PEP):sugar phosphotransferase system (PTS) and is sequestered from the flagellated pole. This delocalization of FapA results in the failure of flagellar formation. When glucose is exhausted, EIIA^{Glc} is phosphorylated. Then FapA is released from EIIA^{Glc} and recruited to the cell pole again to stimulate flagellation. However, the mechanism of how FapA localizes to the cell pole and regulates flagellar assembly remains enigmatic.

In this study, we performed a ligand fishing experiment to identify a factor(s) that contribute to the polar targeting of FapA in *V. vulnificus*. We found that HubP, a polar landmark protein, is the determinant of the polar localization of FapA. We investigated how the spatiotemporal regulation of polar FapA localization, and thereby, flagellar assembly can be achieved depending on the availability of glucose.

Results

FapA directly interacts with HubP

We recently showed that dephosphorylated EIIA^{Glc} inhibits flagellar synthesis by delocalizing FapA from the flagellated pole in *V. vulnificus* (Park *et al.*, 2016). However, it is still unclear as to how FapA is specifically localized to the correct cell pole and how it regulates flagellar synthesis

there. To determine the specific function and to search for a new binding partner of FapA, we performed a ligand fishing experiment using an N-terminally His₆-tagged form of FapA (His-FapA) as bait following the procedure described previously (Park *et al.*, 2016; Choe *et al.*, 2017; Lee *et al.*, 2018). Crude extracts prepared from wild-type *V. vulnificus* MO6-24/O cells grown to stationary phase were mixed with purified His-FapA and then incubated with either glucose to dephosphorylate or PEP to phosphorylate the PTS components (Lee *et al.*, 2019), since the interaction of FapA with EIIA^{Glc} and hence its role in flagellation is strictly dependent on the phosphorylation state of EIIA^{Glc} (Park *et al.*, 2016). After these mixtures were subjected to affinity pull-down assays, we detected a protein band migrating at approximately 20 kDa that eluted only in the fraction containing His-FapA and glucose (Fig. 1A). However, another protein band migrating slower than the 205-kDa molecular mass standard was also detected in the FapA-containing eluates (lane F), but not in the control eluates (lane C), regardless of the presence of glucose and PEP. In-gel tryptic digestion, MALDI-TOF mass spectrometry and peptide mass fingerprinting revealed that the protein band migrating at ~20 kDa corresponded to EIIA^{Glc}, as we expected from our previous finding that only the dephosphorylated form of EIIA^{Glc} interacts with FapA (Park *et al.*, 2016). Interestingly, the protein band above 205 kDa was identified as HubP encoded by VVMO6_00873.

HubP was first named for its proposed function as a polar hub in *V. cholerae* (Yamaichi *et al.*, 2012). *V. vulnificus* HubP is a large (~213 kDa), acidic (pI ~ 3.3)

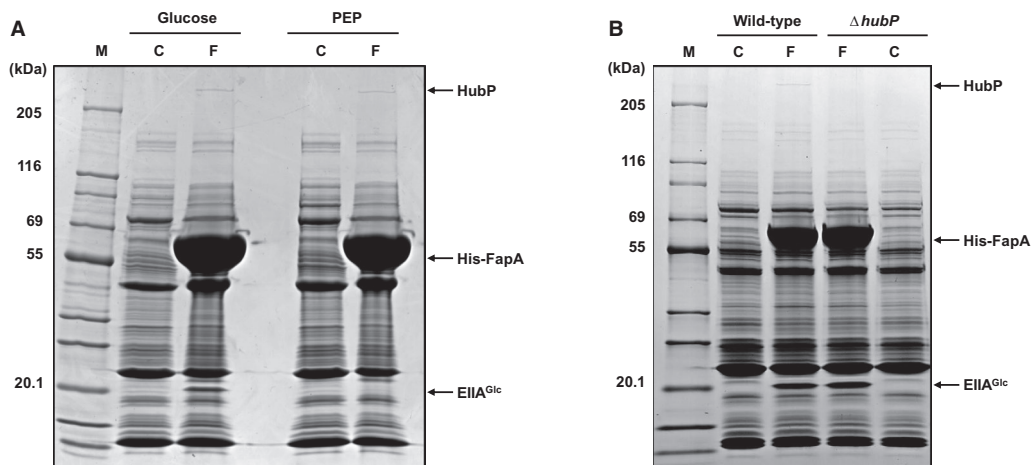


Fig. 1. Ligand fishing experiment to identify proteins interacting with FapA. Ligand fishing experiments were carried out using His₆-tagged FapA (His-FapA) attached to TALON metal affinity resin as bait as described in the experimental procedures.

A. A crude extract prepared from wild-type *V. vulnificus* MO6-24/O cells was mixed with 50 μ l TALON metal-affinity resin (Takara Bio) in the presence of buffer C (control, C) or 500 μ g of His-FapA (F). Glucose or PEP was added to dephosphorylate or phosphorylate EIIA^{Glc}, respectively, as indicated.

B. Crude extract from wild type or Δ hubP *V. vulnificus* was mixed with TALON resin in the presence of buffer C (C) or 350 μ g of His-FapA (F). These mixtures were subjected to affinity chromatography and proteins bound to each column were analyzed by SDS-PAGE and staining with Coomassie brilliant blue R. The protein bands specifically bound to His-FapA are indicated by arrows. M, EzWay Protein Blue MW Marker (KOMA BIOTECH).

transmembrane protein consisting of multiple domains (Supporting information Fig. S1). Its N-terminus consists of a signal peptide, a LysM domain and a single transmembrane domain. The LysM domain is known to bind peptidoglycan in *Pseudomonas aeruginosa* (Semmler *et al.*, 2000; Wehbi *et al.*, 2011) and is required for the polar localization of HubP in *V. cholera* and *Shewanella putrefaciens* (Yamaichi *et al.*, 2012; Rossmann *et al.*, 2015). The C-terminal cytoplasmic region of *V. vulnificus* HubP is composed of five imperfect 83-amino-acid repeats (~30 amino acids in each repeat are acidic) and a FimV C-terminal domain (Buensuceso *et al.*, 2016). HubP, like its binding partner FapA, is conserved in the families *Vibrionaceae* and *Photobacteriaceae* (Supporting information Table S1). Even though *V. vulnificus* HubP is significantly larger than other HubP proteins, *V. vulnificus* HubP shares ~47% amino acid sequence identity with its orthologs in *V. cholerae* and *V. alginolyticus* (Supporting information Fig. S1).

To confirm that the large protein interacting with FapA is HubP, ligand fishing experiments were performed again using TALON metal affinity resin charged with His-FapA as bait. TALON resin charged with His-FapA was incubated with crude extracts of wild-type *V. vulnificus* MO6-24/O and its isogenic *hubP* mutant cells, and then FapA-binding proteins from the two extracts were compared. While both the two protein bands corresponding to EIIA^{Glc} and HubP were detected in the eluate from the column loaded with a mixture of His-FapA and the wild-type cell extract, the protein band above 205 kDa was not detected in the eluate from the column loaded with a mixture of His-FapA and the *hubP* mutant extract (Fig. 1B), indicating that the protein band above 205 kDa was indeed HubP.

The C-terminal cytosolic domain of HubP is sufficient for the interaction with FapA

Given that FapA is a cytosolic protein (Park *et al.*, 2016) and distinct cytoplasmic portions of HubP are required for the polar targeting of the partner proteins in *V. cholerae* (Yamaichi *et al.*, 2012), we reasoned that the cytoplasmic C-terminal domain of HubP would be sufficient to bind FapA in *V. vulnificus*. To verify this assumption, we generated expression vectors for two HubP mutant constructs: HubP Δ (1-657) and HubP Δ (1-1266), in which the N-terminal 657 and 1266 amino acids were deleted respectively (Fig. 2A). When the crude extract prepared from *E. coli* expressing the HubP Δ (1-657) construct was mixed with various amounts of purified His-FapA and then subjected to protein affinity pull-down assays using TALON resin, the amount of HubP Δ (1-657) co-eluted with His-FapA increased as the amount of His-FapA added to the reaction mixture increased (Fig. 2B).

To exclude the possibility that a stretch of highly acidic residues in the C-terminal imperfect repeats of HubP may contribute to the non-specific electrostatic interaction with any positively charged protein domains, we repeated the interaction assays using His-tagged forms of *V. vulnificus* enzyme I (EI) and the global transcription repressor Mlc in comparison to His-FapA. When a mixture of purified HubP Δ (1-1266) with His-FapA, His-EI or His-Mlc was subjected to protein affinity pull-down assays, only the addition of His-FapA increased the binding of HubP Δ (1-1266) to TALON resin compared to the control without His-tagged bait (Supporting information Fig. S2). These results demonstrate that FapA specifically interacts with the cytoplasmic domain of HubP. It should be noted that HubP and its truncated forms show significantly lower stainability with Coomassie brilliant blue and significantly lower electrophoretic mobility in SDS-PAGE gels than expected from their predicted molecular masses due to their higher contents of acidic residues (Wilson, 1979; Tal *et al.*, 1985; Lee *et al.*, 2013; Guan *et al.*, 2015).

We then monitored the complex formation between FapA and HubP by gel filtration chromatography. We compared the elution profile of a mixture of FapA and HubP Δ (1-1266), whose predicted monomer masses are ~60 and ~75 kDa, respectively, from a gel filtration column (Superose 6 10/300 GL; GE Healthcare Life Sciences) with the elution profiles of individual proteins (Fig. 2C). FapA alone was eluted at approximately 14.36 ml, corresponding to its monomeric form, whereas HubP Δ (1-1266) was eluted at approximately 9.28 ml, indicating that it exists as a multimer. When the mixture of FapA and HubP Δ (1-1266) was subjected to gel filtration chromatography, the FapA peak disappeared, with a concomitant increase in the peak at approximately 9.28 ml. When the gel filtration fractions were analyzed by SDS-PAGE, those eluted at approximately 9.28 ml were resolved into two bands corresponding to FapA and HubP Δ (1-1266) (Fig. 2C), indicating that FapA and HubP can form a complex stable enough to persist during gel filtration chromatography.

HubP is the determinant of polar FapA localization

All *Vibrio* species have single or multiple flagella at the old cell pole (Green *et al.*, 2009; Zhu *et al.*, 2013). We previously showed that FapA is targeted to the flagellated old pole in *V. vulnificus* (Park *et al.*, 2016). It has also been reported that HubP is a marker of the old cell pole (Galli *et al.*, 2017). Given the specific interaction of FapA with HubP, we assessed whether HubP is needed to localize FapA at the old cell pole. We firstly observed whether HubP itself localizes at the *V. vulnificus* cell pole. HubP fused with red fluorescent protein at its C-terminus (HubP-RFP) was ectopically expressed in a strain with an in-frame deletion

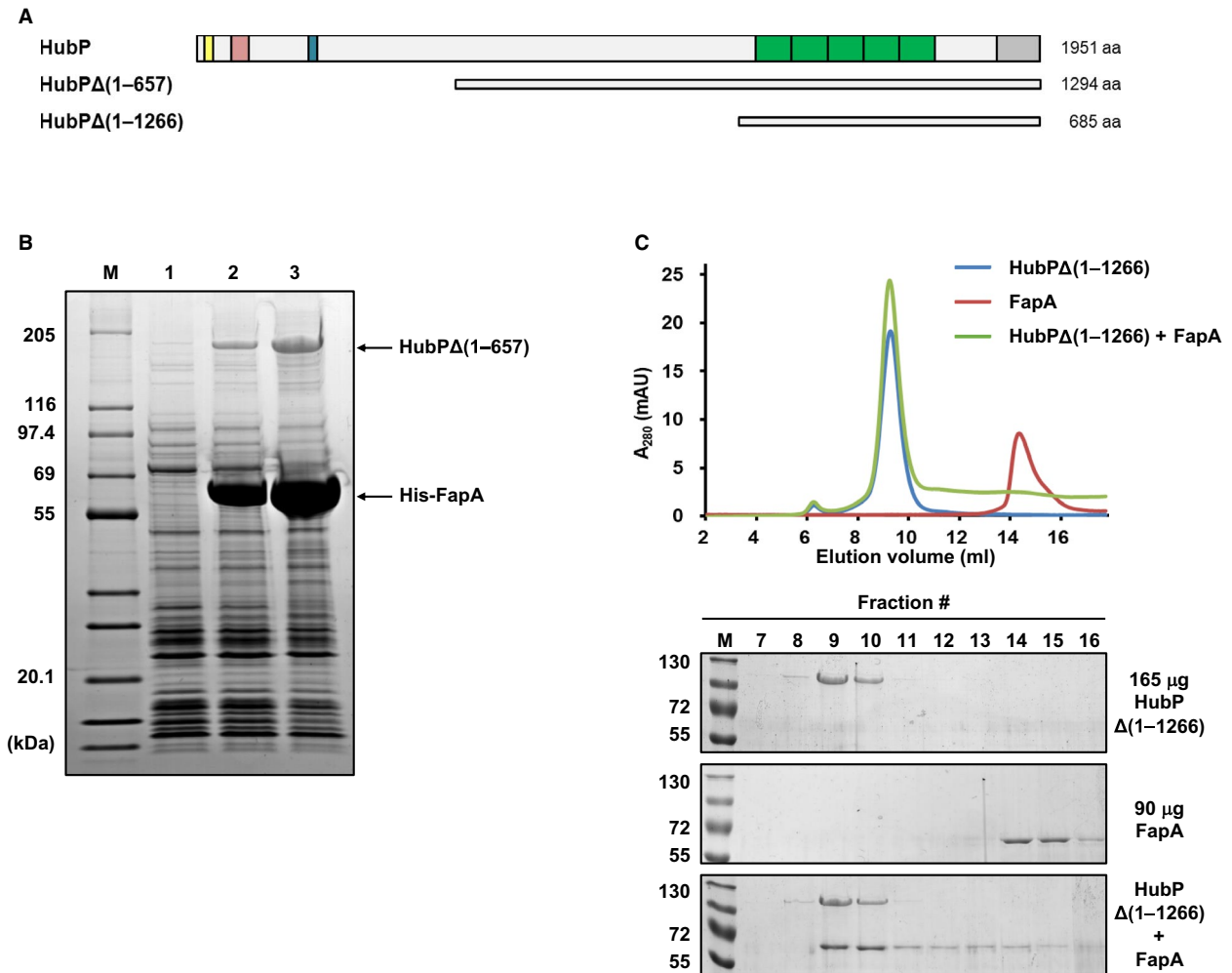


Fig. 2. Specific interaction of FapA with HubP.

A. Schematic presentation of the HubP polypeptide and its N-terminally truncated variants, HubP Δ (1-657) and HubP Δ (1-1266), used in this experiment. Yellow, signal sequence; pink, LysM peptidoglycan-binding domain; blue, transmembrane domain; green, 5 \times repeats; gray, FimV C-terminal domain.

B. An *E. coli* cell extract expressing HubP Δ (1-657) was mixed with various amounts of purified His-FapA (0, 50 and 125 μ g in lanes 1–3 respectively). These mixtures were subjected to His-tag protein affinity pull-down assays using TALON resin. Proteins bound to each column were analyzed by SDS-PAGE and staining with Coomassie brilliant blue R. Lane M, EzWay Protein Blue MW Marker (KOMA BIOTECH).

C. Gel filtration chromatography of HubP Δ (1-1266), FapA and the HubP Δ (1-1266)-FapA complex. Purified HubP Δ (1-1266), FapA or both proteins were loaded onto a Superose 6 10/300 GL column connected to an ÄKTA FPLC system (GE Healthcare Life Sciences). Gel filtration was performed at a flow rate of 0.5 ml min⁻¹ and the elution profiles were monitored by measuring the absorbance at 280 nm. Fractions (1 ml each) were collected, and 20 μ l of each fraction was analyzed by SDS-PAGE using a 10% of gel and stained with Coomassie brilliant blue R. Lane M, PageRulerTM Plus Prestained Protein Ladder (ThermoFisher Scientific). [Colour figure can be viewed at wileyonlinelibrary.com]

of *hubP* and visualized by fluorescence microscopy. As expected from previous reports on HubP localization in other species (Yamaichi *et al.*, 2012; Rossmann *et al.*, 2015; Takekawa *et al.*, 2016), foci of the HubP-RFP fusion protein were clearly observed at the cell poles (Supporting information Fig. S3). The punctate fluorescent foci were still clearly visible at the poles of *fapA* mutant cells, indicating that the failure of flagellar assembly in the *fapA* mutant is not due to an effect on the polar localization of HubP. As demonstrated in our previous study (Park *et al.*, 2016), FapA fused with green fluorescent protein

at its N-terminus (GFP-FapA) formed polar foci in wild-type cells (Fig. 3). However, foci of GFP-FapA were no longer observed in the cell poles and the fluorescence was diffused throughout the cytoplasm in the strain lacking *hubP*. Western immunoblotting of GFP-FapA showed that the stability of GFP-FapA in a strain lacking *hubP* is not significantly different than that in wild type (Supporting information Fig. S4). The polar localization of FapA was restored in the *hubP* deletion strain complemented with the wild-type *hubP* gene in *trans*, indicating that HubP recruits FapA to the cell pole in *V. vulnificus*.

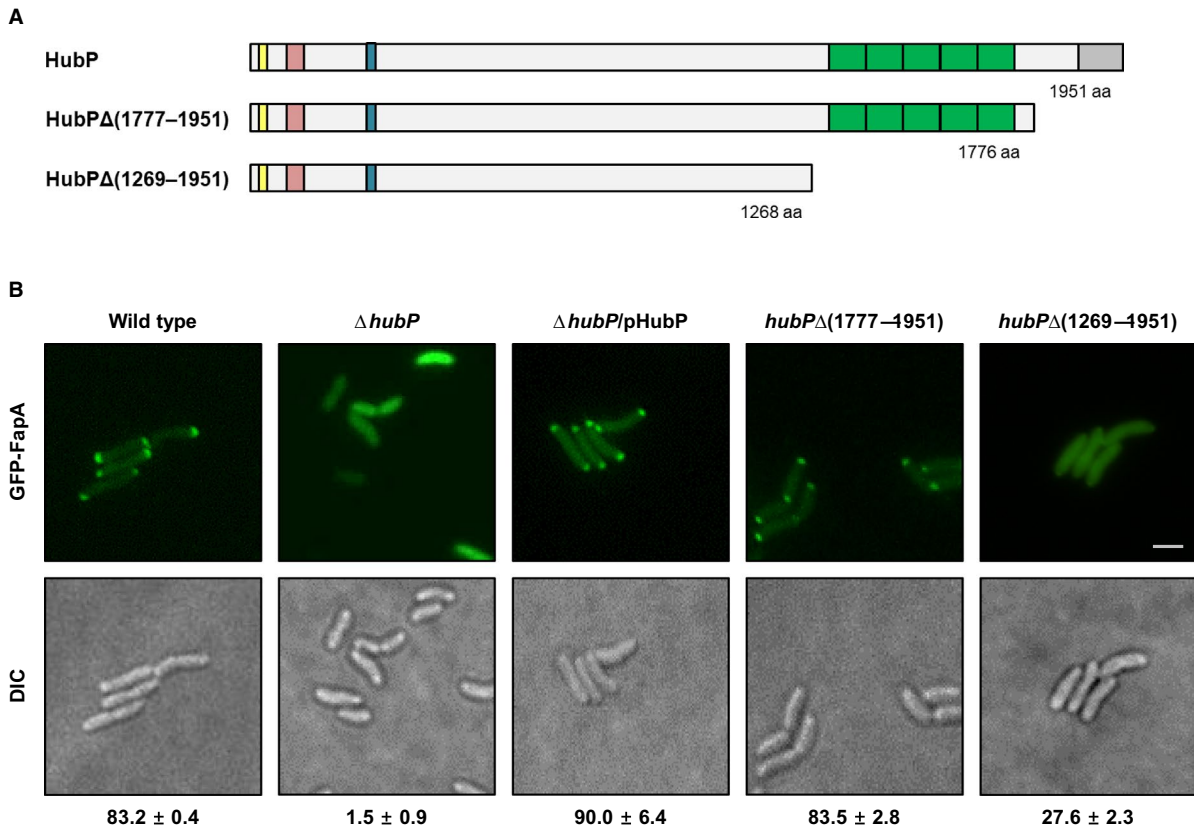


Fig. 3. Requirement of HubP for the polar localization of FapA.

A. Schematic presentation of C-terminally truncated versions of *hubP* constructed to test the role of the HubP C-terminal domain in the polar localization of FapA. The truncation mutations of *hubP* were introduced into the chromosome to the endogenous locus.

B. *V. vulnificus* strains carrying wild type or mutant *hubP* on the chromosome were transformed with an expression vector for the GFP-FapA fusion construct (Park et al., 2016), and the subcellular localization of FapA was monitored by fluorescence microscopy. pHubP is the pJK1113-based expression vector for HubP (pSY021 in Supporting information Table S2). The percentage of cells with polar foci in three independent experiments is presented at the bottom of each panel. Pictures shown are representative fields. Bar, 2 μ m. [Colour figure can be viewed at wileyonlinelibrary.com]

It has been reported that the N-terminal periplasmic LysM domain of HubP is required for its polar targeting in *V. cholerae* and *S. putrefaciens* (Yamaichi et al., 2012; Rossmann et al., 2015). Therefore, we hypothesized that the N-terminal domain of HubP is important for the polar localization of HubP and hence FapA in *V. vulnificus*. To test this hypothesis, RFP was fused to the C-terminus of HubP Δ (1-657), and then this HubP Δ (1-657)-RFP construct was co-expressed with GFP-FapA in a *hubP* deletion strain. When their subcellular localizations were monitored by fluorescence microscopy, neither of the two proteins made foci at the cell pole (Fig. 4). In contrast, green foci were co-localized with red foci at poles in ~90% of the counted cells (669 out of 744 cells) expressing both HubP-RFP and GFP-FapA. These results establish that the association of HubP with the cell pole via its N-terminal domain is required for the polar FapA localization in *V. vulnificus*.

To search for the functionally distinct region of HubP which is crucial for interacting with and guiding the

localization of FapA, we investigated the subcellular localization of GFP-FapA in strains in which the *hubP* gene in the chromosome was mutated (Fig. 3). While deletion of the FimV C-terminal domain (the strain *hubP* Δ (1777-1951) in Fig. 3B) did not affect the ability of HubP to interact with and direct FapA to the cell pole, the polar localization of FapA was significantly decreased in the strain lacking the repeat region of *hubP* (*hubP* Δ (1269-1951)). Additionally, although HubP Δ (303-1718), HubP Δ (665-1951) and HubP Δ (1268-1951) constructs fused to RFP at their C-termini were directed to the cell pole, neither of them could recruit GFP-FapA to the pole, whereas HubP Δ (1726-1951)-RFP could (Fig. 4). These results indicate that the repeat domain of HubP is critical for the interaction with and the polar localization of FapA. Collectively, the N-terminal domain of HubP is primarily responsible for its polar targeting, whereas the repeat domain at its C-terminus is required for the direct interaction with FapA in *V. vulnificus*.

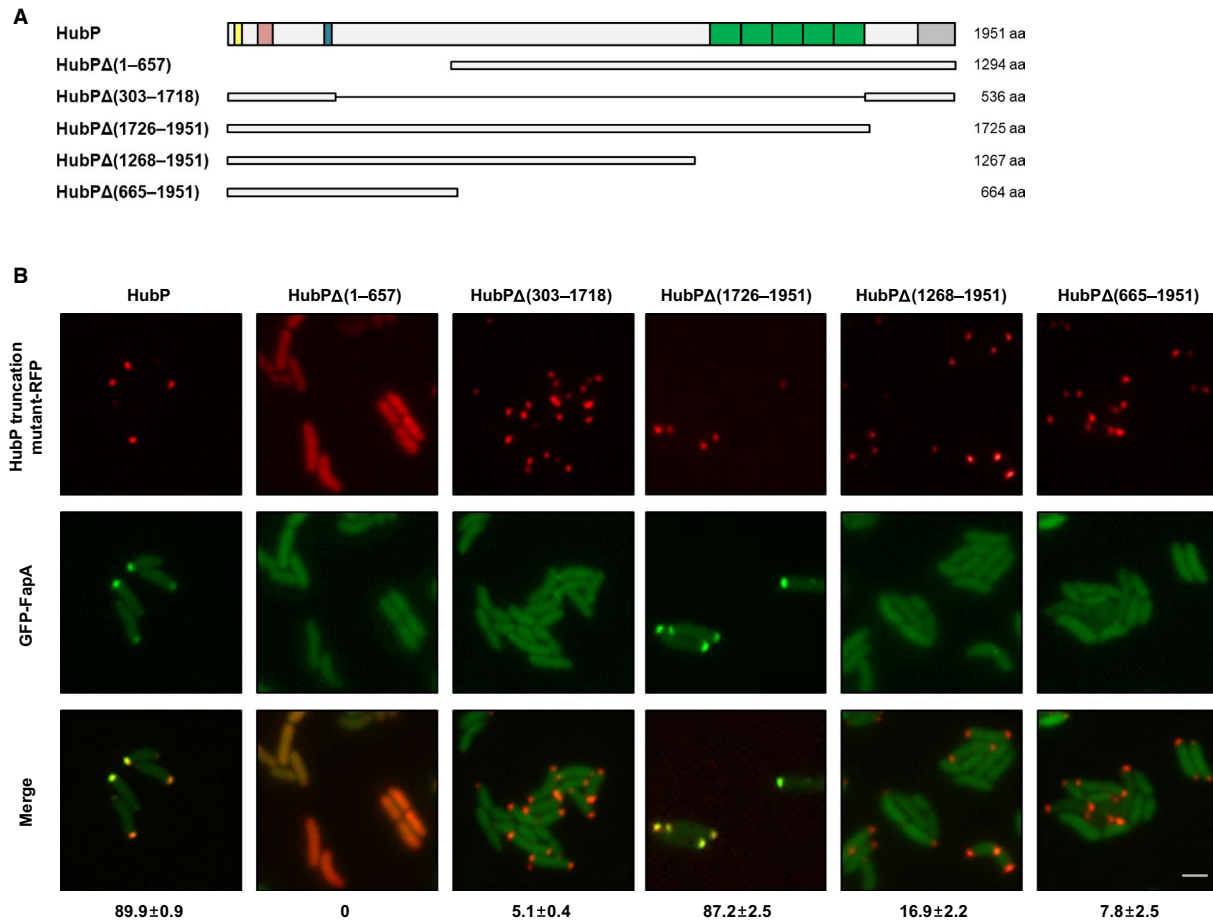


Fig. 4. Effect of deletion mutations of HubP on the polar localization of FapA.

A. Schematic presentation of HubP and its truncated mutants used in this experiment.

B. Wild-type HubP and its truncated forms fused to RFP at their C-termini were co-expressed with GFP-FapA in $\Delta hubP$ *V. vulnificus* cells, and their subcellular localizations were monitored by fluorescence microscopy. The percentage of cells with a polar FapA foci is presented at the bottom of each panel. Representative fields are shown. Bar, 2 μ M. [Colour figure can be viewed at wileyonlinelibrary.com]

All truncated HubP-RFP constructs in plasmids were clearly observed even 5 h after removal of the inducer (arabinose), indicating that these constructs are quite stable. As anticipated, in all cells expressing the LysM-containing HubP constructs fused to RFP, the red fluorescent foci were localized to the cell pole, whereas in all cells expressing HubP Δ (1-657), which is the only HubP construct without the LysM domain, the red fluorescence was diffused throughout the cytoplasm (Fig. 4 and Supporting information Fig. S3). These data indicate that all truncated forms of HubP used in this study are quite stable and all of them carrying the repeat domain are functional in terms of the FapA recruitment in the cell.

HubP controls FapA's distribution and function independently of FlhG

It was previously suggested that polar placement of FapA triggers flagellation in *V. vulnificus* (Park *et al.*, 2016). If

FapA exerts its function in flagellar assembly by interacting with the repeat region of HubP at the cell pole, strains with chromosomal deletions of the repeat domain should display the same flagellation pattern as an *fapA* mutant. As we expected, these two mutant strains exhibited similar motility defects on a soft agar plate (Fig. 5A). Then we questioned whether a strain deleted for the C-terminal extremity of HubP (the FimV C-terminal domain) shows a motility phenotype similar to the wild-type strain. Surprisingly, the *hubP* Δ (1777-1951) mutant strain also showed a motility defect on a swimming plate, similar to the $\Delta fapA$, $\Delta hubP$ and *hubP* Δ (1269-1951) mutant strains (Fig. 5A).

An impairment of swimming ability could be due to loss of chemotaxis or aberrant flagellation. It has been reported that HubP plays important roles in both chemotaxis and flagellar assembly (Yamaichi *et al.*, 2012). For example, targeting of ParC to the cell pole, which facilitates polar localization of chemotactic signaling

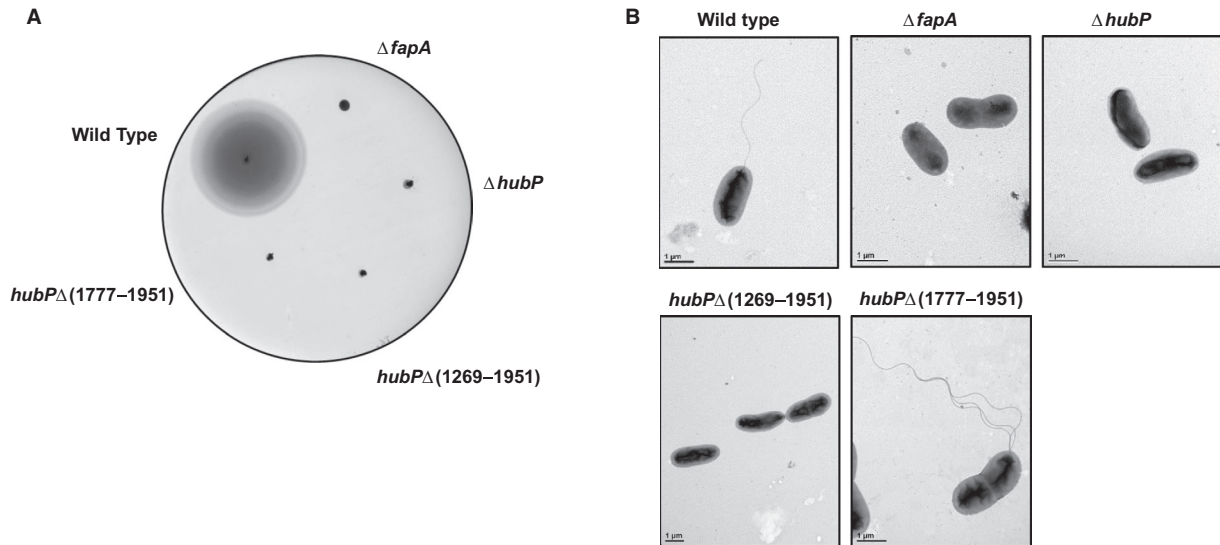


Fig. 5. Swimming motilities and flagellation patterns of wild type and mutant *V. vulnificus* strains.

A. Swimming motility of wild type and *hubP* mutant strains on a 0.3% of agar LBS plate. The plate was incubated at 30°C for 16 h. The $\Delta fapA$ mutant strain served as a negative control.

B. Electron micrographs of the indicated strains grown to exponential phase in LBS medium. Cells were negatively stained with 2% (w/v) uranyl acetate. Bars, 1 μm .

arrays, is dependent on the first 900 amino acids of HubP in *V. cholerae*, although HubP and ParC do not interact with each other (Yamaichi *et al.*, 2012; Ringgaard *et al.*, 2018). Thus, we assumed that the motility defect of the *hubP* $\Delta(1777-1951)$ mutant is unlikely to be associated with ParC. Another factor, ZomB, interacts directly with HubP in *S. putrefaciens* and *V. parahaemolyticus*, and its polar targeting and function are dependent on HubP (Brenzinger *et al.*, 2018). However, little is known about which part of HubP is actually involved in the interaction with ZomB. We expected that *hubP* $\Delta(1777-1951)$ might show a straight-swimming phenotype, as does the *zomB* mutant, if the amino acids 1777-1951 of HubP in *V. vulnificus* is important for the interaction with ZomB. Therefore, motility of the *V. vulnificus hubP* $\Delta(1777-1951)$ strain was tested using the hanging drop method. While wild-type cells exhibited deliberate swimming, no active movement was observed for *hubP* $\Delta(1777-1951)$ mutant cells at all (Data not shown). These results suggest that the extreme C-terminus of HubP is involved in flagellation rather than chemotactic response. Therefore, flagellation patterns were compared among all strains by transmission electron microscopy (Fig. 5B). While the wild-type cells grown in LBS medium had an intact single polar flagellum, the flagellar filament was never observed in cells of the $\Delta fapA$, $\Delta hubP$ and *hubP* $\Delta(1269-1951)$ strains. Interestingly, however, approximately 44.6% of the *hubP* $\Delta(1777-1951)$ cells possessed multiple polar flagella, while only 18.8% of them formed a single flagellum. The other factor, FlhG, was shown to interact directly with the extreme C-terminus of HubP in *V. cholerae* (Yamaichi

et al., 2012). Furthermore, FlhG was shown to affect the number of flagella and *flhG* mutant cells possessed multiple flagella with a motility defect in *V. cholerae* and *S. oneidensis* (Correa *et al.*, 2005; Gao *et al.*, 2015). Therefore, we assumed that the multiple polar flagella and hence a motility defect in the *hubP* $\Delta(1777-1951)$ strain might be due to the loss of its interaction with FlhG. In addition to FapA, FlhG was also diffused throughout the cytoplasm in *hubP* mutant cells (Supporting information Fig. S5), confirming that HubP is the determinant of the polar localization of FapA and FlhG in *V. vulnificus*. We also confirmed that FlhG-RFP could not form foci at the cell pole in the *hubP* $\Delta(1777-1951)$ mutant, while GFP-FapA could (Fig. 3B and Supporting information Fig. S5). These data suggest that the extreme C-terminus of HubP interacts with FlhG, although we do not completely exclude the possible involvement of other HubP client protein(s) in the motility defect of the *hubP* $\Delta(1777-1951)$ mutant. Taken together with the fluorescence (Fig. 3B and Supporting information Fig. S5) and electron micrographic data (Fig. 5B) presented above, these results imply that the repeat domain of HubP is a prerequisite for the interaction with FapA and hence flagellar assembly while the FimV C-terminal domain is required for the regulation of the precise flagella number by interacting with FlhG.

Polar localization of FapA via HubP is crucial for the early stage of flagellar assembly

Several evidences suggest that HubP modulates FapA's distribution and function for flagellar assembly via direct

interaction. It has been reported that the core structure components and organization of the flagellar hook-basal body complex are well conserved in diverse bacterial species (Francis *et al.*, 1994; Terashima *et al.*, 2013; Minamino and Imada, 2015). More than 50 gene products are known to be needed during the highly ordered flagellar assembly process which is temporally and tightly controlled by precise transcriptional mechanisms (Chilcott and Hughes, 2000; McCarter, 2001). In brief, the flagellar assembly starts at the inner structure of the basal body then proceeds to the outer ones, so a deficiency in a gene product which is required for the basal body synthesis will result in a failure of the hook and filament assembly. Therefore, we investigated which step of the flagellar assembly process FapA and HubP were involved in. We purified the membrane fractions containing the flagellar hook-basal body complexes from wild type, *fapA* mutant and *hubP* mutant strains. When the fractions were separated by SDS-PAGE and visualized the proteins by Coomassie brilliant blue R, they displayed similar protein band profiles (Supporting information Fig. S6). To identify the flagellar hook-basal body components from the membrane fractions, each fraction was digested with trypsin and the resulting peptides were analyzed using LC-MS/MS. Then raw data were searched against a UNIPROT protein database of *V. vulnificus* proteins. Twenty-four proteins of the flagellar hook-basal body components were identified in the fraction of the wild-type strain in at least two out of three experiments with high confidence (Table 1), whereas only a few flagellar hook-basal body components were identified in the fractions of $\Delta fapA$ and $\Delta hubP$ mutant strains. A similar profile of flagellar hook-basal body components from the two mutants suggests that the HubP-dependent polar targeting of FapA is important for flagellar assembly. Given that little flagellar proteins were detected in the *fapA* and *hubP* mutants, it could be assumed that the HubP-dependent polar localization of FapA is crucial for the early stage of flagellar assembly. Quantitative RT-PCR (qRT-PCR) analysis revealed that transcription levels of class II flagellar genes encoding the basal body, motor and export apparatus were only slightly, if significantly, changed in the two mutants compared with the wild-type strain (Supporting information Fig. S7). It is noteworthy that class II gene products were not detected in the two mutants in the mass spectrometry analysis, while they were detected in the wild-type strain (Table 1). These data led us to assume that polar targeting of FapA by HubP is likely required for the basal body assembly.

Dephosphorylated EIIA^{Glc} sequesters FapA from HubP

In a previous study, we showed that glucose-specific EIIA^{Glc} is predominantly dephosphorylated in the

presence of glucose, and only dephosphorylated EIIA^{Glc} interacts with FapA and delocalizes it from the pole (Park *et al.*, 2016). We therefore assumed that the HubP-FapA interaction could be affected by the phosphorylation state of EIIA^{Glc}. To test this hypothesis, we examined the effect of the EIIA^{Glc} phosphorylation state on the formation of the HubP-FapA complex by affinity chromatography under various conditions (Fig. 6). Purified His-FapA was mixed with purified HubP Δ (1-657), EIIA^{Glc}, or both. In one set of reaction mixtures containing all three proteins, PEP was supplemented, along with the two general PTS components (enzyme I (EI) and the histidine-containing phosphocarrier protein HPr), to ensure the complete phosphorylation of EIIA^{Glc} (lane 7). Then each mixture was incubated with TALON resin for pull-down assays. After brief washes, proteins bound to the resin were eluted and analyzed by SDS-PAGE (Fig. 6A). The amount of eluted HubP Δ (1-657) significantly increased in the presence of His-FapA, supporting the specific interaction of HubP with FapA (compare lanes 1 and 4). When HubP Δ (1-657) was mixed with His-FapA in the presence of dephosphorylated EIIA^{Glc}, the amount of HubP Δ (1-657) bound to FapA significantly decreased with a concomitant increase in the amount of EIIA^{Glc} bound to FapA (compare lanes 4 and 6), as we assumed. In contrast, when the same mixture was incubated in the presence of PEP to phosphorylate EIIA^{Glc}, formation of the FapA-HubP complex was little affected by EIIA^{Glc} (compare lanes 4 and 7). These data indicate that only the dephosphorylated form of EIIA^{Glc} can interact with FapA and sequester it from HubP. Taken together, our results suggest that dephosphorylated EIIA^{Glc} hinders FapA-mediated flagellation by sequestering FapA from HubP at the cell pole in the presence of glucose (Fig. 6B).

Discussion

The cell poles of rod-shaped bacteria are functionally specialized compartments involved in important cellular processes such as cell cycle regulation, chemotaxis and flagellar motility. Several polar proteins are known to be localized through an interaction with hub-like scaffold proteins anchored to the cell poles (Treuner-Lange and Sogaard-Andersen, 2014). For example, the polar determinant DivIVA in several Gram-positive bacteria assembles at the negative membrane curvature and recruits other binding proteins involved in cell division and chromosome segregation (Lenarcic *et al.*, 2009; van Baarle *et al.*, 2013). In *Caulobacter crescentus*, the polar organizing protein Z, PopZ, interacts directly with ParA and determines its polar localization (Holmes *et al.*, 2016). In *V. cholerae*, HubP anchors three ParA-like ATPase (ParA1, ParC and FlhG) to the cell pole and regulates the polar localization of the chromosome origin,

Table 1. A list of proteins detected by mass spectrometry analysis.

Description	Protein	Accession number	Number of unique peptides		
			WT	Δ <i>fapA</i>	Δ <i>hubP</i>
<i>Flagellar structure</i>					
MS ring	FliF	VVMO6_00818	15	2	–
Export apparatus	FliO	VVMO6_00827	2	2	3
	FliP	VVMO6_00828	1	–	–
	FliE	VVMO6_00817	2	–	–
Rod	FlgB	VVMO6_02266	4	–	–
	FlgC	VVMO6_02265	3	–	–
	FlgF	VVMO6_02262	6	–	–
	FlgG	VVMO6_02261	6	–	–
	FlgI	VVMO6_02259	2	–	–
P ring	FlgH	VVMO6_02260	8	–	–
L ring	MotX	VVMO6_00247	7	1	1
T ring	MotY	VVMO6_02035	13	–	–
H ring	FlgP	VVMO6_02272	8	–	–
	FlgT	VVMO6_02274	17	–	–
Hook	FlgE	VVMO6_02263	4	–	–
Hook-filament junction	FlgK	VVMO6_02257	26	1	1
	FlgL	VVMO6_02256	16	–	–
	FlaF	VVMO6_00807	10	1	1
Flagellin	FlaB/D	VVMO6_00808	4	2	–
		VVMO6_02252			
	FlaA	VVMO6_00809	23	2	–
	FlaE	VVMO6_02251	9	–	–
	FlaC	VVMO6_02255	14	–	–
Filament cap	FliD	VVMO6_00811	13	–	–
<i>House-keeping membrane protein</i>					
Outer membrane protein	OmpU	VVMO6_00583	10	11	11
Outer membrane protein	OmpK	VVMO6_00699	2	3	3
Outer membrane protein	OmpT	VVMO6_00985	2	2	2
Outer membrane integrity protein	TolA	VVMO6_01035	2	3	3
Tol-Pal system periplasmic protein	TolB	VVMO6_01036	20	22	23
Outer membrane channel protein	TolC	VVMO6_04400	20	26	26
Potassium channel protein		VVMO6_01040	9	10	11
Sodium:proton antiporter		VVMO6_02494	8	10	9
Sodium:calcium antiporter		VVMO6_02682	2	2	2
PTS system, fructose-specific IIBC	FruA	VVMO6_03697	4	4	3
PTS system, ascorbate-specific IIC	UlaA	VVMO6_04230	3	4	3
Porin		VVMO6_01837	4	5	4
Glycerol MIP channel, aquaporin	GlpF	VVMO6_00679	10	8	7
Vitamin B12 transporter	BtuB	VVMO6_00146	3	3	3
Penicillin-binding protein 2	PBP2	VVMO6_02312	3	3	3
TonB-dependent heme receptor	HupA	VVMO6_03768	6	9	8
TonB-dependent siderophore receptor	VuuA	VVMO6_04211	12	15	14
Galactose ABC transporter substrate-binding protein	MglB	VVMO6_03135	4	5	6
ATP-dependent zinc metalloprotease	FtsH	VVMO6_00588	19	26	26
Multidrug ABC transporter permease		VVMO6_01651	3	3	3
Cytochrome C		VVMO6_00063	3	6	6

Membrane fractions containing the flagellar hook-basal body complexes were prepared from wild type, *fapA* mutant and *hubP* mutant strains, then each fraction was digested with trypsin and the resulting peptides were analyzed using LC-MS/MS in triplicate.

the chemotaxis machinery and the flagellum (Yamaichi *et al.*, 2012). It has also been reported that HubP recruits non-ParA-like proteins such as SfiA, ZomB and PdeB in *V. alginolyticus* and *S. putrefaciens*, and affects diverse aspects of motility and chemotaxis (Inaba *et al.*, 2017; Brenzinger *et al.*, 2018; Rossmann *et al.*, 2019). In *P. aeruginosa*, FimV, a potential ortholog of HubP, interacts directly with FimL, and modulates type IV pili-mediated

activation of virulence circuits on surface attachment (Inclan *et al.*, 2016).

We have recently shown that the polar localization of FapA is critical for flagellar assembly in *V. vulnificus* (Park *et al.*, 2016). In the absence of glucose, FapA accumulates at the old cell pole so that a flagellum can be assembled there. However, in the presence of glucose, EIIA^{Glc} of the PTS is dephosphorylated and then it delocalizes FapA

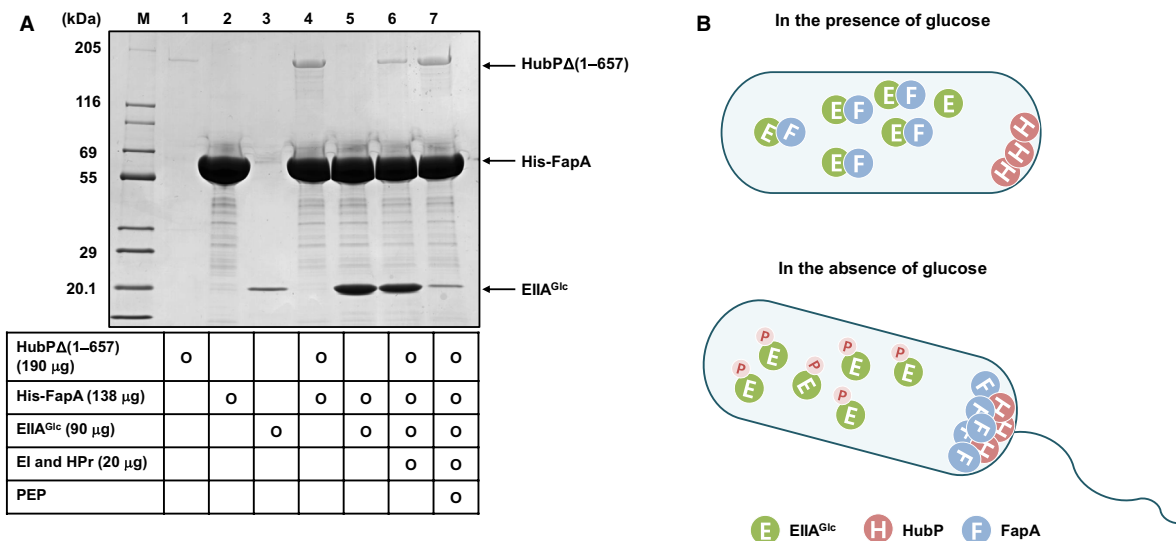


Fig. 6. Sequestration of FapA from HubP by dephosphorylated EIIA^{Glc}.

A. The effect of EIIA^{Glc} on the FapA-HubP complex formation was examined by affinity pull-down analyses under various conditions. Purified HubPA(1-657), His-FapA and EIIA^{Glc} were incubated with 50 µl of TALON resin in different combinations as indicated below each lane, and then subjected to pull-down assays. To phosphorylate EIIA^{Glc}, PEP was added together with enzyme I (EI) and the histidine-containing phosphocarrier protein HPr in lane 7. After a brief wash, proteins bound to the columns were analyzed by SDS-PAGE and staining with Coomassie brilliant blue R. Lane M, EzWay Protein Blue MW Marker (KOMA BIOTECH).

B. A model for the spatiotemporal regulation of the flagella assembly protein FapA in *V. vulnificus*. When glucose is sufficient, glucose-specific enzyme IIA (EIIA^{Glc}) of the PTS is dephosphorylated and sequesters FapA from the polar landmark protein, HubP, by direct interaction. Delocalization FapA hinders the early stage of flagellar assembly, and thereby *V. vulnificus* cells stay in a glucose-rich environment. However, when glucose is exhausted, EIIA^{Glc} is phosphorylated, then FapA dissociates from EIIA^{Glc} and binds to HubP at the pole, where it facilitates flagellar assembly. Therefore, the cells can start swimming to search for a more favorable location. [Colour figure can be viewed at wileyonlinelibrary.com]

from the pole by direct interaction to inhibit flagellation. In this study, we investigated the scaffold protein responsible for the polar accumulation of FapA and found that FapA is localized to the old cell pole by specifically interacting with the polar landmark protein HubP in *V. vulnificus* (Fig. 1). Dephosphorylated EIIA^{Glc} competes with HubP for the interaction with FapA (Fig. 6). Therefore, in a glucose-rich environment, EIIA^{Glc} is dephosphorylated and it sequesters FapA from HubP to stop flagellar assembly and cells stay there. When glucose is exhausted, however, EIIA^{Glc} is phosphorylated and HubP can then recruit FapA to the old cell pole to resume flagellation to seek a better environment (Figs 3 and 6). Therefore, we identify FapA as a new non-ParA-like client of HubP in *V. vulnificus* from this study. Through this spatiotemporal regulation of the polar FapA localization, *V. vulnificus* cells can stay and survive in more favorable environment.

Connections between HubP and *Vibrio* flagellation have been previously reported (Yamaichi *et al.*, 2012; Takekawa *et al.*, 2016). While it appears that the deletion of *hubP* leads to the inhibition of flagellar motility in all *Vibrio* species examined thus far, *hubP* mutants show quite diverse flagellation patterns depending on the species. Approximately 50% of *V. alginolyticus* cells formed multiple flagella in the absence of HubP, whereas the deletion of *hubP* had a modest effect on flagellar number in *V. cholerae* and only 6% of *hubP* mutant cells produced more than a single

flagellum. In *V. vulnificus*, a *hubP* mutant is non-motile and this loss of motility turned out to be due to a complete failure of flagellar assembly (Fig. 5). Purification of hook-basal bodies and mass spectrometry analyses revealed that both the *hubP* and *fapA* mutant lack most flagellar hook-basal body components (Table 1), indicating that the recruitment of FapA to the pole by HubP is the crucial step for the initiation of flagellar assembly in *V. vulnificus*.

Although the overall structure of HubP is conserved among HubP homologs (Supporting information Fig. S1), acidic repeats at the cytoplasmic part of HubP homologs differ in length, copy number and amino acid composition from one another (Yamaichi *et al.*, 2012; Rossmann *et al.*, 2015; Takekawa *et al.*, 2016). Therefore, we assume that the difference in the repeat domains may reflect different client proteins among HubP homologs. HubP consists of multiple domains including the acidic repeat domain and the FimV C-terminal domain (Supporting information Fig. S1). Since the cytoplasmic portions of HubP are required for interaction with its client proteins, it could be assumed that a specific domain might be responsible for the recruitment of a particular client to the cell pole. We justified this assumption by showing that, while FapA interacts with the imperfect repeat region of HubP, the ParA-like protein FlhG binds to the C-terminal extremity of HubP where it regulates the number of flagella (Fig. 3 and Supporting information Fig. S5). Therefore, we demonstrate that HubP

orchestrates flagellar assembly by recruiting FapA and flagella number by recruiting FlhG in *V. vulnificus*. Since it is known that flagellar assembly is temporally controlled and the assembly process is tightly coordinated (Chevance and Hughes, 2008; Minamino and Imada, 2015), we still need to identify the particular step catalyzed by FapA to understand the exact flagellar assembly process in *V. vulnificus*.

Experimental procedures

Bacterial strains, plasmids and culture conditions

Bacterial strains, plasmids and oligonucleotides used in this study are listed in Supporting information Tables S2 and S3. *V. vulnificus* strains were cultured in Luria-Bertani medium supplemented with 2.5% of NaCl (LBS) at 30°C and *E. coli* strains were grown in LB medium at 37°C. The following supplements were added if necessary: kanamycin, 200 µg ml⁻¹ for *V. vulnificus* and 50 µg ml⁻¹ for *E. coli*; ampicillin, 100 µg ml⁻¹ for *E. coli*; chloramphenicol, 2 µg ml⁻¹ for *V. vulnificus* and 20 µg ml⁻¹ for *E. coli*; isopropyl-β-D-1-thiogalactopyranoside (IPTG), 1 mM; and L-arabinose, 0.02%. Constructions of various *hubP* mutants were generated by allelic exchange using pDM4-based plasmid as described previously (Park *et al.*, 2016).

All expression vectors for HubP and its truncation mutants were constructed using standard PCR-based cloning procedures and verified by sequencing. To construct pSY021 to overexpress HubP, the *hubP* gene amplified by PCR using primers JY010 and JY012 (Supporting information Table S3) were digested with NcoI and Sall and inserted into the corresponding sites of pJK1113. Then, the *bla* gene in this plasmid was replaced with a chloramphenicol resistance marker as described previously (Park *et al.*, 2016). The *cat* gene PCR product and the linearized PCR product of the plasmid except the *bla* gene were combined by EZ Fusion™ Cloning kit (Enzyomics), resulting in the pSY021.

To construct expression vectors for RFP fusion proteins, each ORF was amplified by PCR and combined with the PCR product of the pJK1113-based RFP fusion vector pSY008 amplified by inverse PCR with the primers JW023 and JW024 (Supporting information Table S3) using EZ-Fusion™ Cloning kit.

Protein expression and purification

Proteins with N-terminal His-tags cloned into pET vectors were overexpressed in *E. coli* BL21 (DE3)/pLysS or ER2566, and purified using TALON metal-affinity resin (Takara Bio) according to the manufacturer's instructions. Proteins bound to TALON resin were eluted with 200 mM of imidazole, and then chromatographed on a HiLoad 16/600 Superdex 200 pg column (GE Healthcare Life Sciences) equilibrated with buffer A (50 mM of Tris-HCl, pH 7.5, 100 mM of NaCl, 0.05% of β-mercaptoethanol and 5% of glycerol). EIIA^{Glc} without a His-tag was purified as described previously (Park *et al.*, 2016). Truncated forms of untagged HubP were cloned into pET vectors (pSY016 and pSY017) and overexpressed in *E. coli* BL21 (DE3)/pLysS (Supporting information Table S2). Harvested cells were resuspended in buffer B (50 mM

of Tris-HCl, pH 7.5, 50 mM of NaCl, 1 mM of dithiothreitol, 1 mM of ethylenediaminetetraacetic acid and 5% of glycerol) and disrupted by three passages through a French pressure cell at 8,000 psi. After centrifugation at 100,000 × *g* at 4°C for 40 min, the supernatant was applied to a Mono Q 10/100 column (GE Healthcare Life Sciences). Protein elution was performed using a 12-column volume gradient of 0.5–1.5 M NaCl in buffer B at a flow rate of 1.5 ml min⁻¹. The fractions containing the HubP truncation mutants were concentrated, and then chromatographed on a HiLoad 16/60 Superdex 200 pg column (GE Healthcare Life Sciences) equilibrated with buffer A to achieve a higher purity (>90%).

Ligand fishing experiment using metal affinity chromatography

Wild type or *hubP* mutant *V. vulnificus* MO6-24/O cells grown overnight in LBS medium were harvested, washed and resuspended in buffer C (50 mM of sodium phosphate, pH 8.0, 200 mM of KCl and 5 mM of imidazole). Cells were disrupted by three passages through a French pressure cell at 8,000 psi. After centrifugation at 10,000 × *g* at 4°C for 15 min, the supernatant was mixed with either buffer C as a control or purified His-tagged FapA (His-FapA). Each mixture was then incubated with TALON metal affinity resin (Takara Bio) at 4°C for 15 min. After three washes with buffer C, the bound proteins were eluted with 2× SDS loading buffer. The eluted protein samples (20 µl each) were analyzed by SDS-PAGE using 4–20% gradient gel (KOMA BIOTECH) and staining with Coomassie brilliant blue R. Protein bands specifically bound to the His-FapA were excised from the gel, and tryptic in-gel digestion and peptide mapping were carried out as previously described (Lee *et al.*, 2007; Kim *et al.*, 2010; Park *et al.*, 2013).

Motility assay in soft agar plates and transmission electron microscopy

V. vulnificus strains were grown in LBS to OD₆₀₀ = 0.5 and spotted onto an LBS soft agar plate (LBS medium containing 0.3% of agar). Then swimming mobility assays were performed as described previously (Park *et al.*, 2016). *V. vulnificus* cells were negatively stained with 2% of uranyl acetate and examined by transmission electron microscopy as described previously (Park *et al.*, 2016).

Visualization of fluorescent fusion proteins in live cells

Fluorescence microscopy was carried out essentially as described previously (Park *et al.*, 2016). An aliquot (2 µl) of culture was spotted on an agarose pad (1% of agarose in phosphate-buffered saline). Microscopy was performed using a Deltavision Restoration Microscope System (GE Healthcare Life Sciences).

Isolation of membrane fraction containing the flagellar hook-basal body complex

Isolation of the flagellar basal bodies was performed as described previously (Terashima *et al.*, 2006; 2010) with

some modifications. Cells grown in LBS to OD₆₀₀ = 1.0 were harvested, washed and resuspended in sucrose buffer (50 mM of Tris-HCl, pH 7.5, 0.5 M of Sucrose). The suspended cells were converted into spheroplasts by adding lysozyme and EDTA to final concentrations of 0.1 mg ml⁻¹ and 5 mM respectively. The spheroplasts were lysed by adding Triton X-100 to a final concentration of 1% (w/v) and incubated for 1 h. To reduce the viscosity of the lysed spheroplasts, MgSO₄ and DNase I were added to final concentrations of 10 mM and 0.1 mg ml⁻¹, respectively, incubated at 30°C for 30 min. Unlysed cells and cellular debris were removed by centrifugation at 12,000 × *g* at 4°C for 20 min, and polyethylene glycol 8000 and NaCl were added to the lysate to final concentrations of 2% and 100 mM respectively. The suspension was incubated at 4°C for 1 h, and then centrifuged at 27,000 × *g* at 4°C for 30 min. The pellet was resuspended in 6 ml of TED buffer (10 mM of Tris-HCl, pH 8.0, 5 mM of EDTA, 0.1% (w/v) of dodecyl maltoside). The suspension was centrifuged at 1,000 × *g* at 4°C for 15 min to remove cellular debris. The supernatant was centrifuged 100,000 × *g* at 4°C for 30 min, and the pellet was resuspended in 200 μl of TED buffer. To dissociate the flagellar filaments into monomeric flagellin, the suspension was diluted 30-fold in 50 mM of glycine-HCl, pH 3.5 containing 0.1% (w/v) of dodecyl maltoside and shaken at 30°C for 60 min. After the sample was centrifuged at 1,000 × *g* at 4°C for 15 min, the supernatant was centrifuged at 150,000 × *g* at 4°C for 40 min. The pellet was resuspended in 100 μl of TED buffer.

Sample preparation for LC-MS/MS analysis

Membrane fractions containing flagellar basal bodies (~100 μg protein each) were dissolved in 100 μl of 50 mM of ammonium bicarbonate, reduced with 10 mM of DTT at 60°C for 60 min and alkylated with 25 mM of iodoacetamide at room temperature for 60 min in the dark. The samples were then digested with trypsin at 37°C overnight. Total peptide concentration was measured by Qubit assay (Thermo Fisher Scientific) and the digested peptides were desalted using a macro spin column (Harvard Apparatus), following the manufacturer's protocols respectively. The desalted peptide samples were dried under vacuum and reconstituted with 0.1% (v/v) formic acid/water for LC-MS/MS analysis.

LC-MS/MS analysis

Mass spectrometric analyses of the trypsin-digested samples were performed using an Orbitrap Fusion Lumos mass spectrometer (Thermo Fisher Scientific) equipped with a nano-electrospray source (EASY-Spray Sources, Thermo Fisher Scientific) and an Easy nanoLC 1200 (Thermo Fisher Scientific) in the Korea Basic Science Institute (KBSI). The peptides (5 μg of total proteins) were loaded and separated on an analytical C18 column (75 μm × 50 cm PepMap RSLC, Thermo Fisher Scientific) at a flow rate of 300 nl min⁻¹. The mobile phases A and B were composed of 0 and 80% (v/v) of acetonitrile containing 0.1% of formic acid respectively. The LC gradient began with 2% B for 1 min and was linearly

ramped up to 6% B for 1 min, 10% B for 30 min, 50% B for 120 min and 100% B for 1 min. The column was washed with 100% B for 8 min and re-equilibrated with 2% B for 20 min before the next run. During the chromatographic separation, the Orbitrap Fusion Lumos was operated in data-dependent mode with 3 s cycle time. The voltage applied to produce an electrospray was 2 kV. Full scan MS1 spectra (40–1600 m z⁻¹) were acquired in the Orbitrap for a maximum ion injection time of 100 ms at a resolution of 120,000 and an automatic gain control (AGC) target value of 2 × 10⁵. MS2 spectra were acquired in the Orbitrap mass analyzer at resolution of 30,000 with high-energy collision dissociation (HCD) of 27% normalized collision energy and AGC target value of 5 × 10⁴ with maximum ion injection time of 54 ms. Previously fragmented ions were excluded for 15 s. Data acquisition was processed using Xcalibur 2.2 and Tune 2.7 software.

Database searching

The MaxQuant quantitative proteomics tool (version 1.5.2.8) was introduced to process raw files, as stated before (Jang *et al.*, 2017). Spectra were searched against *V. vulnificus* protein database (139,418 sequences, downloaded on 27/06/17) from UNIPROT. Common contaminants (245 sequences) were also included in the database. An equal number of decoy sequences were used to estimate the false discovery rate (FDR) from the spectra. The digestion enzyme was specified as trypsin with up to two missed cleavages. Methionine oxidation (+15.9949), protein N-terminal acetylation (+42.0106) and N-terminal methionine formylation (+27.9919) were specified as variable modifications and cysteine carbamidomethylation (+57.0215) was set as a fixed modification. A fragment ion tolerance of 0.5 Da, a maximum precursor ion tolerance of 6 ppm after recalibration, and all other parameters were used as default. Identifications were filtered to curate a dataset with less than 1% of FDR at both the peptide and the protein level.

Acknowledgements

We thank Hyeong-In Ham for critical reading of the manuscript. This work was supported by National Research Foundation Grants NRF-2015R1A2A1A15053739 and NRF-2018R1A5A1025077 funded by the Ministry of Science and ICT.

Conflict of interest

The authors declare that they have no conflict of interest with the contents of this article.

Author contributions

SP, CRL, KHL and YJS designed the study. SP, JY, CRL, JYL and KSJ performed the experiments. SP, JY, CRL, KSJ, and YJS analyzed the data. SP, JY, CRL, YRK, KHL and YJS wrote the paper.

Data availability statement

The data that support the findings of this study are available from the corresponding author upon reasonable request.

References

- van Baarle, S., Celik, I.N., Kaval, K.G., Bramkamp, M., Hamoen, L.W. and Halbedel, S. (2013) Protein–protein interaction domains of *Bacillus subtilis* DivIVA. *Journal of Bacteriology*, **195**, 1012–1021.
- Brenzinger, S., Pecina, A., Mrusek, D., Mann, P., Volse, K., Wimmi, S., et al. (2018) ZomB is essential for flagellar motor reversals in *Shewanella putrefaciens* and *Vibrio parahaemolyticus*. *Molecular Microbiology*, **109**, 694–709.
- Buensuceso, R.N., Nguyen, Y., Zhang, K., Daniel-Ivad, M., Sugiman-Marangos, S.N., Fleetwood, A.D., et al. (2016) The conserved tetratricopeptide repeat-containing C-terminal domain of *Pseudomonas aeruginosa* FimV is required for its cyclic AMP-dependent and -independent functions. *Journal of Bacteriology*, **198**, 2263–2274.
- Chevance, F.F. and Hughes, K.T. (2008) Coordinating assembly of a bacterial macromolecular machine. *Nature Reviews Microbiology*, **6**, 455–465.
- Chilcott, G.S. and Hughes, K.T. (2000) Coupling of flagellar gene expression to flagellar assembly in *Salmonella enterica* serovar typhimurium and *Escherichia coli*. *Microbiology and Molecular Biology Reviews*, **64**, 694–708.
- Choe, M., Park, Y.H., Lee, C.R., Kim, Y.R. and Seok, Y.J. (2017) The general PTS component HPr determines the preference for glucose over mannitol. *Scientific Reports*, **7**, 43431.
- Correa, N.E., Peng, F. and Klose, K.E. (2005) Roles of the regulatory proteins FlhF and FlhG in the *Vibrio cholerae* flagellar transcription hierarchy. *Journal of Bacteriology*, **187**, 6324–6332.
- Francis, N.R., Sosinsky, G.E., Thomas, D. and DeRosier, D.J. (1994) Isolation, characterization and structure of bacterial flagellar motors containing the switch complex. *Journal of Molecular Biology*, **235**, 1261–1270.
- Galli, E., Paly, E. and Barre, F.X. (2017) Late assembly of the *Vibrio cholerae* cell division machinery postpones septation to the last 10% of the cell cycle. *Scientific Reports*, **7**, 44505.
- Gao, T., Shi, M., Ju, L. and Gao, H. (2015) Investigation into FlhFG reveals distinct features of FlhF in regulating flagellum polarity in *Shewanella oneidensis*. *Molecular Microbiology*, **98**, 571–585.
- Green, J.C., Kahramanoglou, C., Rahman, A., Pender, A.M., Charbonnel, N. and Fraser, G.M. (2009) Recruitment of the earliest component of the bacterial flagellum to the old cell division pole by a membrane-associated signal recognition particle family GTP-binding protein. *Journal of Molecular Biology*, **391**, 679–690.
- Guan, Y., Zhu, Q., Huang, D., Zhao, S., Jan Lo, L. and Peng, J. (2015) An equation to estimate the difference between theoretically predicted and SDS PAGE-displayed molecular weights for an acidic peptide. *Scientific Reports*, **5**, 13370.
- Holmes, J.A., Follett, S.E., Wang, H., Meadows, C.P., Varga, K. and Bowman, G.R. (2016) *Caulobacter* PopZ forms an intrinsically disordered hub in organizing bacterial cell poles. *Proceedings of the National Academy of Sciences of the United States of America*, **113**, 12490–12495.
- Inaba, S., Nishigaki, T., Takekawa, N., Kojima, S. and Homma, M. (2017) Localization and domain characterization of the SflA regulator of flagellar formation in *Vibrio alginolyticus*. *Genes to Cells*, **22**, 619–627.
- Inclan, Y.F., Persat, A., Greninger, A., Von Dollen, J., Johnson, J., Krogan, N., et al. (2016) A scaffold protein connects type IV pili with the Chp chemosensory system to mediate activation of virulence signaling in *Pseudomonas aeruginosa*. *Molecular Microbiology*, **101**, 590–605.
- Jang, K.S., Park, M., Lee, J.Y. and Kim, J.S. (2017) Mass spectrometric identification of phenol-soluble modulins in the ATCC® 43300 standard strain of methicillin-resistant *Staphylococcus aureus* harboring two distinct phenotypes. *European Journal of Clinical Microbiology and Infectious Diseases*, **36**, 1151–1157.
- Kim, Y.J., Ryu, Y., Koo, B.M., Lee, N.Y., Chun, S.J., Park, S.J., et al. (2010) A mammalian insulin homolog is regulated by enzyme IIA^{Glc} of the glucose transport system in *Vibrio vulnificus*. *FEBS Letters*, **584**, 4537–4544.
- Laloux, G. and Jacobs-Wagner, C. (2014) How do bacteria localize proteins to the cell pole? *Journal of Cell Science*, **127**, 11–19.
- Lee, C.R., Cho, S.H., Yoon, M.J., Peterkofsky, A. and Seok, Y.J. (2007) *Escherichia coli* enzyme IANtr regulates the K⁺ transporter TrkA. *Proceedings of the National Academy of Sciences of the United States of America*, **104**, 4124–4129.
- Lee, C.R., Park, Y.H., Kim, Y.R., Peterkofsky, A. and Seok, Y.J. (2013) Phosphorylation-dependent mobility shift of proteins on SDS-PAGE is due to decreased binding of SDS. *Bulletin of the Korean Chemical Society*, **34**, 2063–2066.
- Lee, J.W., Park, Y.H. and Seok, Y.J. (2018) Rsd balances (p)ppGpp level by stimulating the hydrolase activity of SpoT during carbon source downshift in *Escherichia coli*. *Proceedings of the National Academy of Sciences of the United States of America*, **115**, E6845–E6854.
- Lee, C.R., Park, Y.H., Min, H., Kim, Y.R. and Seok, Y.J. (2019) Determination of protein phosphorylation by polyacrylamide gel electrophoresis. *Journal of Microbiology*, **57**, 93–100.
- Lenarcic, R., Halbedel, S., Visser, L., Shaw, M., Wu, L.J., Errington, J., et al. (2009) Localisation of DivIVA by targeting to negatively curved membranes. *EMBO Journal*, **28**, 2272–2282.
- McCarter, L.L. (2001) Polar flagellar motility of the *Vibrionaceae*. *Microbiology and Molecular Biology Reviews*, **65**, 445–462.
- Minamino, T. and Imada, K. (2015) The bacterial flagellar motor and its structural diversity. *Trends in Microbiology*, **23**, 267–274.
- Park, Y.H., Lee, C.R., Choe, M. and Seok, Y.J. (2013) HPr antagonizes the anti- σ^{70} activity of Rsd in *Escherichia coli*. *Proceedings of the National Academy of Sciences of the United States of America*, **110**, 21142–21147.
- Park, S., Park, Y.H., Lee, C.R., Kim, Y.R. and Seok, Y.J. (2016) Glucose induces delocalization of a flagellar

- biosynthesis protein from the flagellated pole. *Molecular Microbiology*, **101**, 795–808.
- Ringgaard, S., Yang, W., Alvarado, A., Schirner, K. and Briegel, A. (2018) Chemotaxis arrays in *Vibrio* species and their intracellular positioning by the ParC/ParP system. *Journal of Bacteriology*, **200**, e00793–17.
- Rossmann, F., Brenzinger, S., Knauer, C., Dörrich, A.K., Bubendorfer, S., Ruppert, U., *et al.* (2015) The role of FlhF and HubP as polar landmark proteins in *Shewanella putrefaciens* CN-32. *Molecular Microbiology*, **98**, 727–742.
- Rossmann, F.M., Rick, T., Mrusek, D., Sprankel, L., Dörrich, A.K., Leonhard, T., *et al.* (2019) The GGDEF domain of the phosphodiesterase PdeB in *Shewanella putrefaciens* mediates recruitment by the polar landmark protein HubP. *Journal of Bacteriology*, **201**, e00534–18.
- Schuhmacher, J.S., Thormann, K.M. and Bange, G. (2015) How bacteria maintain location and number of flagella? *FEMS Microbiology Reviews*, **39**, 812–822.
- Semmler, A.B.T., Whitchurch, C.B., Leech, A.J. and Mattick, J.S. (2000) Identification of a novel gene, *fimV*, involved in twitching motility in *Pseudomonas aeruginosa*. *Microbiology*, **146**, 1321–1332.
- Takekawa, N., Kwon, S., Nishioka, N., Kojima, S. and Homma, M. (2016) HubP, a polar landmark protein, regulates flagellar number by assisting in the proper polar localization of FlhG in *Vibrio alginolyticus*. *Journal of Bacteriology*, **198**, 3091–3098.
- Tal, M., Silberstein, A. and Nusser, E. (1985) Why does Coomassie Brilliant Blue R interact differently with different proteins? A partial answer. *Journal of Biological Chemistry*, **260**, 9976–9980.
- Terashima, H., Fukuoka, H., Yakushi, T., Kojima, S. and Homma, M. (2006) The *Vibrio* motor proteins, MotX and MotY, are associated with the basal body of Na⁺-driven flagella and required for stator formation. *Molecular Microbiology*, **62**, 1170–1180.
- Terashima, H., Koike, M., Kojima, S. and Homma, M. (2010) The flagellar basal body-associated protein FlgT is essential for a novel ring structure in the sodium-driven *Vibrio* motor. *Journal of Bacteriology*, **192**, 5609–5615.
- Terashima, H., Li, N., Sakuma, M., Koike, M., Kojima, S., Homma, M. and Imada, K. (2013) Insight into the assembly mechanism in the supramolecular rings of the sodium-driven *Vibrio* flagellar motor from the structure of FlgT. *Proceedings of the National Academy of Sciences of the United States of America*, **110**, 6133–6138.
- Treuner-Lange, A. and Søgaard-Andersen, L. (2014) Regulation of cell polarity in bacteria. *Journal of Cell Biology*, **206**, 7–17.
- Wehbi, H., Portillo, E., Harvey, H., Shimkoff, A.E., Scheurwater, E.M., Howell, P.L. and Burrows, L.L. (2011) The peptidoglycan-binding protein FimV promotes assembly of the *Pseudomonas aeruginosa* Type IV pilus secretin. *Journal of Bacteriology*, **193**, 540–550.
- Wilson, C.M. (1979) Studies and critique of Amido Black 10B, Coomassie Blue R, and Fast Green FCF as stains for proteins after polyacrylamide gel electrophoresis. *Analytical Biochemistry*, **96**, 263–278.
- Yamaichi, Y., Bruckner, R., Ringgaard, S., Moll, A., Cameron, D.E., Briegel, A., *et al.* (2012) A multidomain hub anchors the chromosome segregation and chemotactic machinery to the bacterial pole. *Genes & Development*, **26**, 2348–2360.
- Zhu, S., Kojima, S. and Homma, M. (2013) Structure, gene regulation and environmental response of flagella in *Vibrio*. *Frontiers in Microbiology*, **4**, 410.

Supporting Information

Additional supporting information may be found online in the Supporting Information section at the end of the article